Molecular Imaging and Biology
https://doi.org/10.1007/s11307-023-01826-5

RESEARCH ARTICLE

# Use of Electron Paramagnetic Resonance (EPR) to Evaluate Redox Status in a Preclinical Model of Acute Lung Injury

**Hanan B. Elajaili[1] · Nathan M. Dee[1] · Sergey I. Dikalov[2] · Joseph P. Y. Kao[3] · Eva S. Nozik[1]**

Received: 28 December 2022 / Revised: 3 May 2023 / Accepted: 8 May 2023


## Abstract

**Purpose** Patients with hyper- vs. hypo-inflammatory subphenotypes of acute respiratory distress syndrome (ARDS) exhibit different clinical outcomes. Inflammation increases the production of reactive oxygen species (ROS) and increased ROS contributes to the severity of illness. Our long-term goal is to develop electron paramagnetic resonance (EPR) imaging of lungs *in vivo* to precisely measure superoxide production in ARDS in real time. As a first step, this requires the development of *in vivo* EPR methods for quantifying superoxide generation in the lung during injury, and testing if such superoxide measurements can differentiate between susceptible and protected mouse strains.

**Procedures** In WT mice, mice lacking total body extracellular superoxide dismutase (EC-SOD) (KO), or mice overexpressing lung EC-SOD (Tg), lung injury was induced with intraperitoneal (IP) lipopolysaccharide (LPS) (10 mg/kg). At 24 h after LPS treatment, mice were injected with the cyclic hydroxylamines 1-hydroxy-3-carboxy-2,2,5,5-tetramethylpyrrolidine hydrochloride (CPH) or 4-acetoxymethoxycarbonyl-1-hydroxy-2,2,5,5-tetramethylpyrrolidine-3-carboxylic acid (DCP-AM-H) probes to detect, respectively, cellular and mitochondrial ROS – specifically superoxide. Several probe delivery strategies were tested. Lung tissue was collected up to one hour after probe administration and assayed by EPR.

**Results** As measured by X-band EPR, cellular and mitochondrial superoxide increased in the lungs of LPS-treated mice compared to control. Lung cellular superoxide was increased in EC-SOD KO mice and decreased in EC-SOD Tg mice compared to WT. We also validated an intratracheal (IT) delivery method, which enhanced the lung signal for both spin probes compared to IP administration.

**Conclusions** We have developed protocols for delivering EPR spin probes *in vivo*, allowing detection of cellular and mitochondrial superoxide in lung injury by EPR. Superoxide measurements by EPR could differentiate mice with and without lung injury, as well as mouse strains with different disease susceptibilities. We expect these protocols to capture real-time superoxide production and enable evaluation of lung EPR imaging as a potential clinical tool for subphenotyping ARDS patients based on redox status.

**Keywords** Lung · Acute respiratory distress syndrome · Superoxide · Mitochondria · Spin probe · Spin trap

## Introduction

The most severe form of acute lung injury (ALI), acute respiratory distress syndrome (ARDS), is a principal cause of life-threatening illness in both adults and children. Prior to 2020, more than 190,000 cases of ARDS were reported annually in the US with in-hospital mortality of 38.5% and significant long-term morbidity for survivors. The incidence and mortality of ARDS greatly increased due to the COVID-19 pandemic, highlighting the seriousness of this disease process [1–3]. Unfortunately, despite decades of research into effective treatments, the high mortality of ARDS has remained largely unchanged and the long-term burden in

✉ Eva S. Nozik
eva.nozik@cuanschutz.edu

[1] Pediatric Critical Care Medicine, University of Colorado Anschutz Medical Campus, 12700 E. 19th Ave., B131, Aurora, CO 80045, USA

[2] Department of Medicine, Division of Clinical Pharmacology, Vanderbilt University Medical Center, Nashville, TN, USA

[3] Center for Biomedical Engineering and Technology, and Department of Physiology, University of Maryland School of Medicine, Baltimore, MD, USA

Published online: 16 May 2023

survivors is increasingly being recognized [3]. Emerging research in ARDS establishes the urgent need to define subphenotypes of patients (hypo-inflammatory and hyper-inflammatory) that account for the variable responses to therapies [4–7].

Inflammation leads to the increased production of reactive oxygen species (ROS) and consequent oxidative stress, which has been recognized as a key feature of ARDS [8]. Unfortunately, despite decades of research supporting the role of ROS in ARDS pathogenesis, trials of antioxidant treatments failed to reduce the mortality of this disease [9–15]. One barrier to this work is that currently available measures of oxidative stress are imprecise owing to technical limitations, for example, the use of indirect markers of oxidative stress such as malondialdehyde and 4-hydroxynonenal (MDA + 4-HNE), products of lipid peroxidation, as an indirect measure of the cumulative lipid peroxidation in plasma as a surrogate for lung ROS production [16, 17]. Given the relationship between inflammation and oxidative stress, and the evidence that the level of inflammation may differentiate high-risk patients that will benefit from therapeutic interventions, there is an urgent need to develop improved tools to precisely detect ROS production in the lung.

Electron paramagnetic resonance (EPR) spectroscopy is unique as a method for detecting, identifying, and quantitating free radicals. It is thus a crucial analytical tool in the field of free radical and redox biology. Detection of short-lived free radicals *in vivo* by EPR requires the use of special molecular probes – so-called "spin traps" that react with the transient radicals to generate more stable, longer-lived radicals that can be quantified by EPR. Specifically, cyclic hydroxylamine probes react with superoxide with high sensitivity to generate a stable nitroxide product, which is easily identified and quantified by EPR spectroscopy (S1). In more advanced applications, probes that are cell-permeant or that are designed to accumulate in the mitochondria permit determination of superoxide in different cellular compartments. Injecting the probes into live mice enables one to quantify superoxide production *in vivo*.

We aim to harness the power of EPR to determine lung superoxide production in an inflammatory model of acute lung injury. In this study, we developed different strategies to deliver the molecular probes *in vivo* to enhance the EPR signal. We used two probes that detect total cellular and mitochondrial superoxide, respectively. Selectivity of the probes for superoxide was confirmed by the elimination of the signal by pharmacologic or genetic delivery of superoxide dismutase [18, 19]. After the probes react with superoxide *in vivo*, the resulting signal was quantified in excised lung by EPR. We evaluated three mouse strains: 1) WT mice; 2) a susceptible mouse strain lacking a key lung antioxidant enzyme, extracellular superoxide dismutase (EC-SOD, or *sod3*); and 3) a protected mouse strain with lung-specific overexpression of EC-SOD. Our findings allowed us to determine if the EPR measurements could distinguish between mouse strains with different disease risks.

## Materials and Methods

### Mouse Model

Animal studies were approved by the University of Colorado Denver (Aurora, CO) Institutional Animal Care and Use Committee. We tested different strains with susceptibility or resistance to LPS-induced injury due to alterations in the expression of EC-SOD. The susceptible mouse strain lacks total body EC-SOD (KO) [20]. The protected transgenic mouse strain overexpresses EC-SOD (Tg) specifically in the lung, as the *sod3* transgene is driven by the surfactant protein C promoter in type II alveolar epithelial cells [21]. All strains are bred onto the C57BL/6 mouse background and evaluated along with WT C57BL/6 control mice.

Periodic immunoblots verify the absence of EC-SOD in KO mice and the presence of human EC-SOD in TG mice. Mice are routinely genotyped depending on the breeding strategy. All EC-SOD KO breeding pairs are genotyped prior to use to confirm that all offspring will be total body EC-SOD KO mice. Moreover, since heterozygous TG mice are crossed with WT mice to generate lung-overexpressing TG (heterozygous) mice for experiments, all offspring are genotyped to determine if the individual is a TG mouse or WT littermate prior to use.

### Injury Model

Lung injury was induced with a single dose of intraperitoneal (IP) lipopolysaccaride (LPS) (*E. coli* O55; Sigma) (10 mg/kg). Mice were treated with LPS or PBS controls and evaluated at 24 h. After delivering the probes *in vivo* to live mice, the mice were euthanized with $CO_2$ and cervical dislocation. The chest cavity was opened and the lungs were flushed with 5 ml of cold PBS via the right ventricle. Lungs were collected for EPR measurements as described below.

### Delivery of Molecular Probes

Cyclic hydroxylamines 1-hydroxy-3-carboxy-2,2,5,5-tetramethylpyrrolidine hydrochloride (CPH) (ENZO) or 4-acetoxymethoxycarbonyl-1-hydroxy-2,2,5,5-tetramethylpyrrolidine-3-carboxylic acid (DCP-AM-H) (gift of Igor Kirilyuk, Novosibirsk Institute of Organic Chemistry, Russia) [19] were used in this study. Stock solutions of cyclic hydroxylamines were prepared in Krebs–Henseleit buffer (KHB) containing 25 μM deferoxamine mesylate salt and 5 μM sodium diethyldithiocarbamate (Sigma Aldrich) and

bubbled with nitrogen for 30 min to remove dissolved oxygen. The stock solutions were freshly prepared daily and kept on ice.

At 24 h after LPS treatment, mice were injected with the probes CPH or DCP-AM-H to detect cellular and mitochondrial superoxide, respectively. CPH and DCP-AM-H have no EPR signal of their own. However, reaction of CPH with superoxide forms the stable nitroxide radical CP•, and the reaction of superoxide with DCP-AM-H and intracellular cleavage of the acetoxymethyl (AM) ester generates the nitroxide DCP•. CP• and DCP• both exhibit robust and distinct EPR spectra that are readily detected and quantified. Accumulation of DCP-AM-H in the mitochondria was validated in a previous study using mice overexpressing the mitochondrial isoform of superoxide dismutase (SOD2) [19]. To minimize autoxidation, stock solutions of the probes were first dissolved in degassed KHB containing the following chelators, 25 μM deferoxamine mesylate salt and 5 μM sodium diethyldithiocarbamate for a final stock concentration of 9 mM for CPH and 2.5 mM for DCP-AM-H.

CPH (0.18 mg, 90 μl of 9 mM CPH stock) was delivered as an intraperitoneal bolus, followed immediately by 1 subcutaneous (SQ) dose (0.27 mg, 135 μl of 9 mM CPH stock) [22]. Based on an average mouse bodyweight of 20 g, the dose was selected to provide 9 mg/kg IP and 13.5 mg/kg SQ; this protocol is designated "IP/SQ". We also tested 2 other delivery strategies to optimize the EPR signal: 1) CPH was given as described above, but with a second SQ dose 30 min after the initial administration (deisgnated "IP/2SQ"); 2) CPH was administered intratracheally (IT) (0.2 mg, 100 μL of 9 mM CPH). DCP-AM-H was given as a single IP or IT dose (100 μL of 2.5 mM stock). Lungs were harvested 1 h after the end of IP/SQ, 30 min after the end of IP/2SQ, and 5 min after IT delivery (S2). Lungs were kept on ice and EPR measurements were performed 2 h after the harvest. Injections with the spin probe were staggered and alternated between treatments (PBS/LPS) to ensure that the difference observed was not confounded by time.

### EPR Measurments

The EPR measurments were performed on an X-band (ca. 9.6 GHz) spectrometer (EMXnano, Bruker Corp.). Fresh lung tissue (8–10 mg) was placed in the tissue cell accessory and EPR measurements were performed at room temperature with the following EPR acquisition parameters: microwave frequency = 9.65 GHz; center field = 3432 G; modulation amplitude = 2.0 G; sweep width = 80 G; microwave power = 19.9 mW; total number of scans = 10; sweep time = 12.11 s; and time constant = 20.48 ms. Owing to the difficulty of recovering the tissue from the tissue cell accessory to perform quantitative assays, results were normalized to the weight of tissue and not to the lung protein.

### Statistical Analysis

Data were analyzed using Prism (GraphPad Software, La Jolla, CA, USA) by unpaired t-test or ordinary one-way ANOVA. Post-hoc analysis was performed using Tukey's test when significant differences were found between groups. Data are expressed as mean ± SEM. Significance was defined as $p < 0.05$.

## Results

### Optimizing Probe Delivery to Detect Cellular Superoxide in the Lungs of LPS-Treated and Control Mice

We aimed to establish a protocol to assay superoxide production *in vivo* in mice after LPS exposure. We first tested a published protocol that used 2 doses of CPH – 0.18 mg IP followed immediately by a single 0.27 mg dose SQ (protocol IP/SQ) [23]. We then repeated the protocol with the IP injection followed immediately by an SQ injection and a second SQ injection 30 min later (protocol IP/2SQ). The additional SQ dose enhanced the EPR signal, as shown in Fig. 1a. Representative EPR spectra resulting from the two dosing regimens are shown in Fig. 1b.

### Cellular Superoxide was Higher in the Lungs of LPS-Treated EC-SOD KO Mice and Lower in Mice Overexpressing Lung EC-SOD Compared to WT

To determine whether this protocol could differentiate mice with different disease risks due to the expression levels of EC-SOD [20, 21, 24–41], we exposed mice with different lung injury susceptibility to LPS. We compared a susceptible mouse strain lacking an important first-line antioxidant defense, EC-SOD (KO), and a protected mouse strain overexpressing EC-SOD (Tg). Relative to WT, LPS-induced superoxide was higher in the KO mice and lower in the Tg mice (Fig. 2a, b).

### Increased Mitochondrial Superoxide in LPS-Treated Lung Compared to the Control

LPS induces mitochondrial damage in the lung [42]. We sought to measure mitochondrial superoxide production *in vivo* after LPS challenge by injecting the mitochondrially-targeted probe, DCP-AM-H. Higher mitochondrial superoxide was detected in the lungs from LPS-treated mice compared to control mice (Fig. 3a). The increase in mitochondrial superoxide production after LPS treatment was exacerbated in mice lacking EC-SOD (Fig. 3b).

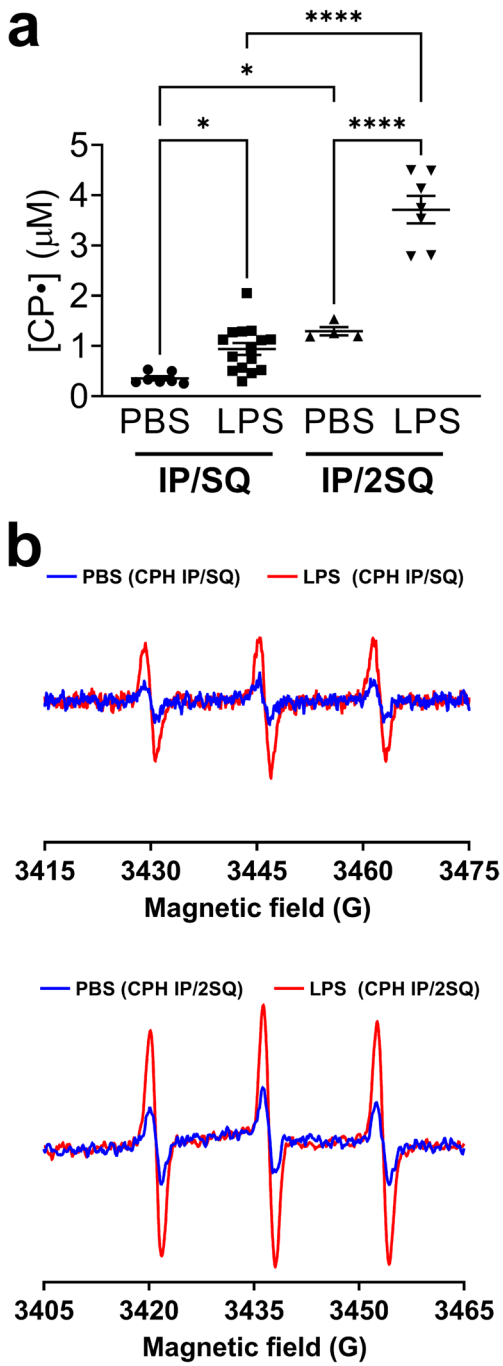


**Fig. 1** Optimization of spin probe delivery method to detect cellular superoxide in the lung of LPS-treated and control mice. Mice were treated with LPS (10 mg/kg, intraperitoneal (IP) injection). After 24 h mice were injected with CPH with two dosing strategies: 1) Concurrent IP and subcutaneous (SQ) injection, followed by lung harvest 1 h later (protocol IP/SQ); 2) Concurrent IP and SQ injection plus a second SQ injection 30 min later, with lung harvest after a further 30 min (protocol IP/2SQ). See Materials and Methods for details. (**a**) Concentration of nitroxide CP• in the lungs of PBS- and LPS-treated mice. (**b**) EPR spectra of nitroxide CP• in the lungs of mice that were PBS-treated (blue traces) and LPS-treated (red traces) following the two dosing strategies. Measurements at X-band were done at room temperature. Data expressed as mean ± SEM; *$p < 0.05$, ****$p < 0.0001$ ($n = 4$–15)

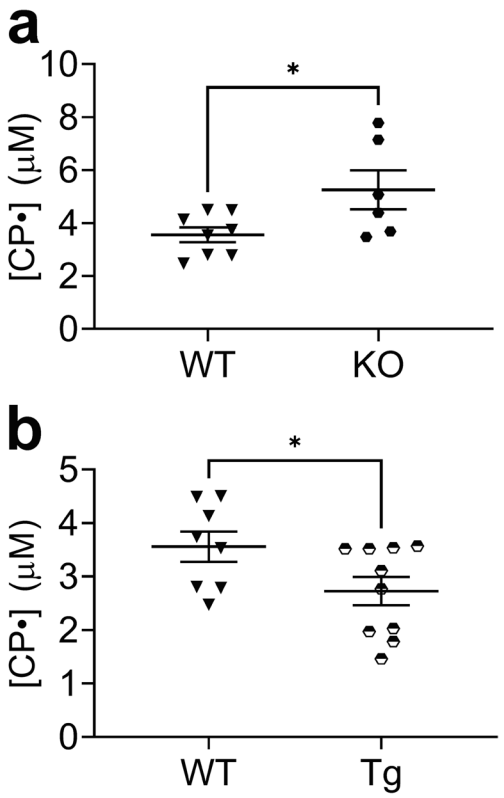


**Fig. 2** Cellular superoxide was higher in the lungs of LPS-treated EC-SOD KO mice and lower in the lungs of LPS-treated mice overexpressing lung EC-SOD compared to WT. Mice were treated with LPS (10 mg/kg, intraperitoneal (IP) injection). After 24 h mice were injected with CPH (protocol IP/2SQ: concurrent IP and SQ injection plus a second SQ injection 30 min later, with lung harvest after another 30 min). See Materials and Methods for details. Concentration of nitroxide CP• was assayed by EPR **a**) in lungs of EC-SOD KO vs WT mice; (**b**) in EC-SOD-overexpressing Tg vs WT mice. Data expressed as mean ± SEM; *$p < 0.05$ ($n = 6$–10)

## Intratracheal (IT) Delivery of Molecular Probes Enhances the EPR Signal

To enhance the signal further, we tested the direct, intratracheal delivery of the probe to the lung. A significant signal enhancement was observed compared to the IP/2SQ strategy for both CPH and DCP-AM-H, as shown in Figs. 4a and b, respectively. The IT delivery method still allowed differentiation of injured and uninjured lungs by both CPH and DCP-AM-H, as demonstrated in Fig. 5a and b, respectively.

## Discussion

Excessive free radical production is implicated in numerous diseases including ARDS. In this study, we developed new protocols for using compartment-selective cyclic hydroxylamine probes with EPR spectroscopy to

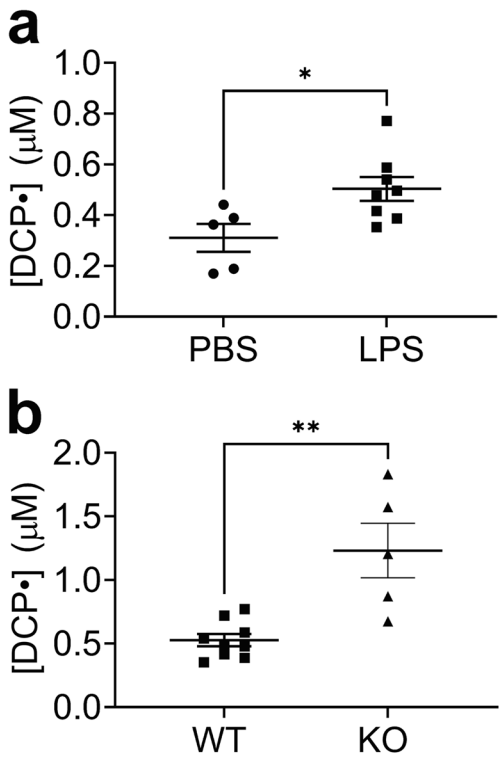


**Fig. 3** Higher mitochondrial superoxide in the lungs of LPS-treated mice compared to control and higher in EC-SOD KO mice compared to WT. Mice were treated with LPS (10 mg/kg, intraperitoneal (IP) injection). After 24 h mice were injected with DCP-AM-H (IP) with lung harvest 1 h later. See Materials and Methods for details. (**a**) Concentration of nitroxide DCP• in the lungs of PBS-treated mice and LPS-treated mice. (**b**) Concentration of nitroxide DCP• in the lungs of LPS-treated EC-SOD KO and WT mice. Data expressed as mean ± SEM; $*p < 0.05$ ($n = 5$–9)

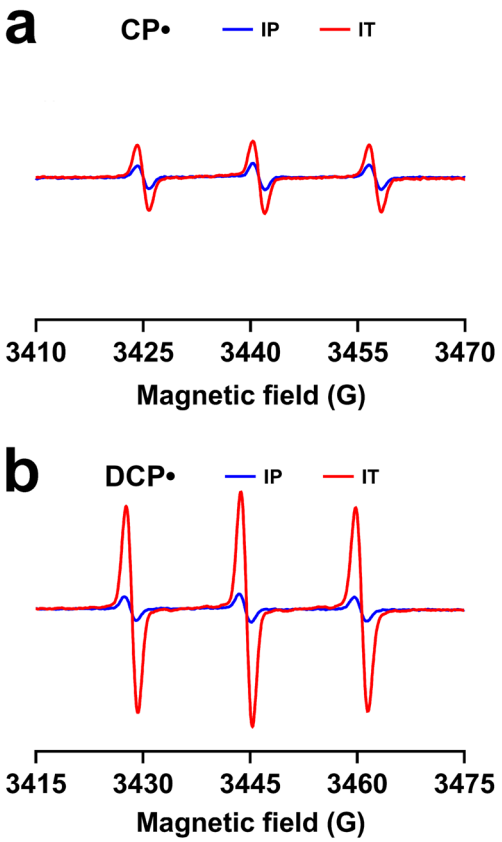


**Fig. 4** Intratracheal (IT) delivery of probes enhances the EPR signals arising from CPH and DCP-AM-H. Mice were treated with LPS (10 mg/kg, intraperitoneal (IP) injection). After 24 h CPH or DCP-AM-H probe was delivered intratracheally (IT); 5 min thereafter lungs were harvested. See Materials and Methods for details. (**a**) EPR spectra of nitroxide CP• in lungs from mice treated with CPH IT vs IP. (**b**) EPR spectra of nitroxide DCP• in lungs from mice treated with DCP-AM-H IT vs IP

rigorously evaluate superoxide production in the lung following LPS exposure. Cellular and mitochondrially-targeted probes were delivered to live mice and lung tissue was collected for EPR measurements at room temperature. Both cellular and mitochondrial superoxide in lung increased at 24 h after LPS. The increase in lung superoxide was aggravated in mice lacking EC-SOD and was attenuated in mice overexpressing lung EC-SOD. Mitochondrial superoxide also increased in mice lacking EC-SOD compared to WT mice. The EPR spectroscopic signal was first enhanced by using an IP injection followed by 2 SQ doses, and further increased by IT delivery. These protocols improve the utility of EPR in detecting the production of superoxide.

The first important outcome of this study is that we developed and validated protocols that combine EPR molecular probes with EPR spectroscopy to detect the production of superoxide in different cellular compartments. By injecting the mice with hydroxylamine probes that accumulated selectively in the cytosol or mitochondria, the protocols enabled the measurement of superoxide production in these distinct compartments under control conditions and following LPS. This provided the advantage of capturing superoxide generation *in vivo* rather than in excised lung tissue *ex vivo*. Using mice that lack EC-SOD or overexpress lung EC-SOD [21, 24–41], we were able to differentiate the superoxide levels between susceptible and resistant mouse strains. While EPR spectroscopy has been the gold standard for detecting paramagnetic species such as organic free radicals, this study both advances the use of EPR spectroscopy for biological measurements and provides advantages over other methods used to evaluate ROS and oxidative stress. For example, fluorescent probes of ROS are commercially available and include dihydroethidium (DHE) and dichlorodihydrofluorescein (DCFH). However, fluorescent probes are light-sensitive, undergo facile autoxidation, and form multiple nonspecific oxidation products that require the use of high-performance liquid chromatography (HPLC)

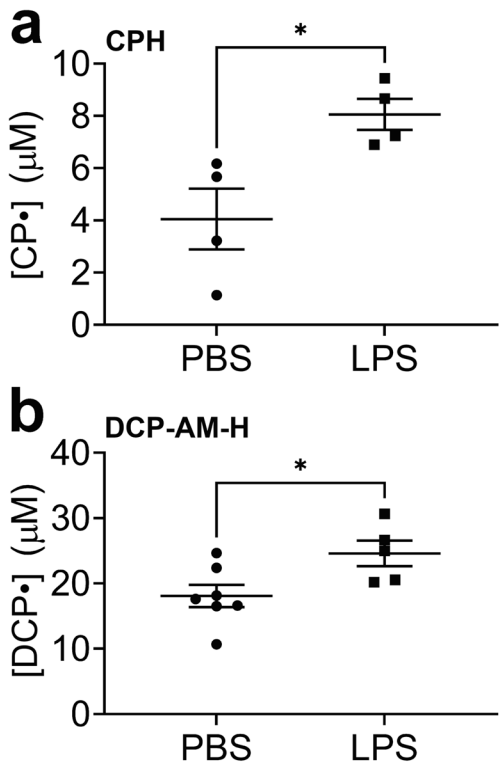


**Fig. 5** Intratracheal (IT) probe delivery permits detection of increased cellular and mitochondrial superoxide in the lungs of LPS-treated mice compared to the control. Mice were treated with LPS (10 mg/kg intraperitoneal (IP) injection). After 24 h CPH or DCP-AM-H probe was delivered intratracheally (IT); 5 min thereafter lungs were harvested. See Materials and Methods for details. (**a**) Concentration of nitroxide CP• in the lungs of PBS-treated or LPS-treated mice. (**b**) Concentration of nitroxide DCP• in the lungs of PBS-treated and LPS-treated mice. Data expressed as mean ± SEM; $*p < 0.05$ ($n = 4$–7)

for identification [43]. Although HPLC-based detection of DHE oxidation products is selective for superoxide and has been tested in multiple organs after LPS, it cannot be used in imaging [44]. A study reported the injection of CPH *in vivo* post-LPS, followed by EPR measurements at liquid nitrogen temperature [45]. Our current study advances this work by using hydroxylamine probes, validating their utility in different mouse strains, and detecting superoxide production in intact tissue at room temperature.

Cyclic hydroxylamines can be susceptible to metal-catalyzed oxidation; therefore the probes were prepared in deoxygenated buffer containing metal chelators to minimize autoxidation. The cyclic hydroxylamine probes are selective, though not specific, for superoxide – for example, they can react with peroxynitrite, the reaction product of superoxide with nitric oxide. The best evidence of the probes' selectivity for superoxide in biological systems is the fact that the EPR signals are abolished when superoxide dismutase is delivered pharmacologically or genetically [18, 19]. While we did not differentiate between extracellular and intracellular superoxide with CPH, our results show that changing the extracellular redox environment changes intracellular and mitochondrial superoxide levels. This finding is consistent with our recently published study in bleomycin-induced lung injury, where altered EC-SOD content impacts mitochondrial superoxide production and metabolism [46]. This does not indicate that EC-SOD directly lowers superoxide in other compartments, but more likely demonstrates the protection against intracellular or mitochondrial processes indirectly. Currently, there are several other studies supporting the concept that alterations in EC-SOD can impact mitochondrial function. Kusuyama and colleagues showed that inducible loss of EC-SOD in the placenta prevented exercise-induced AMPK activation and downstream glucose metabolism in the fetal hepatocyte [39]. It was also reported that EC-SOD overexpression promoted the survival of SH-SY5Y cells by maintaining mitochondrial homeostasis [40]. These advances establish a foundation that supports the future application of these protocols to *in vivo* imaging. Furthermore, our protocols can be utilized to detect compartmental superoxide production in other organs and disease models.

The second key outcome of this study is that we significantly enhanced the signal by delivering the molecular probes by intratracheal instillation. This improvement in signal-to-noise ratio (S/N) is significant because this protocol overcomes the sensitvity limitation in using low-frequncy EPR imaging of the lung *in vivo*, which is a longterm goal of this work. Low-frequency EPR spectroscopy is essential to *in vivo* EPR imaging because the radio waves used for imaging penetrate into tissues much better at lower frequency. However, the improved tissue penetration at lower frequency comes at the price of decreased sensitivity [47, 48]. Improving S/N substantially decreases the time required for imaging and improves image quality for the same data acquisition time. While IT administration is established for drug delivery, to our knowledge this is the first study to use this method to deliver imaging probes to the lung. The enhancement in S/N through the direct delivery of the probes to the lungs (IT delivery approach) confirmed that the signal intensity depends on not only the amount of ROS generated but also the local concentration of the hydroxylamine probe. Our findings are essential advances supporting the goal of EPR imaging the lung. We propose that a robust, real-time imaging modality to detect lung oxidative stress could be a useful tool to identify hyper-inflamed patients with ARDS and guide trials in the future.

In summary, the most severe form of ALI, ARDS, is a serious medical problem. Unfortunately, despite decades of research in search of effective treatments, the high mortality of ARDS has remained largely unchanged, and the long-term burden in survivors is increasingly being recognized. In this study, we develop EPR methodology to detect free

radical production in damaged lungs in a murine model of ALI. The methods demonstrated in this study enable the capture of superoxide in excised lung in an ALI injury model. This study is an important advance toward *in vivo* imaging of acute lung injury in live mouse and, ultimately, to assessing the redox state of the lungs of ARDS patients to guide interventions.

**Supplementary Information** The online version contains supplementary material available at https://doi.org/10.1007/s11307-023-01826-5.

**Acknowledgements** This work was supported by 1R33 HL157907-01 (ESN, SE),1R35HL139726-01 (ESN) and R01HL144943 (SD). The authors thank Dr. Sandra Eaton and Dr. Gareth Eaton (University of Denver) for helpful discussions, and Laura Hernandez-Lagunas and Janelle Posey (University of Colorado Denver) for technical support.

**Authors Contributions** Elajaili, Hanan B. Design and perform experiments, analyze data, interpret results, and write manuscript.
Dee, Nathan M. Perform experiments and edit manuscript.
Dikalov, Sergey I. Interpret results and edit manuscript.
Kao, Joseph P. Y. Interpret results and edit manuscript.
Nozik, Eva S. Design experiments, analyze data, interpret results, and edit manuscript.
All authors critically reviewed the manuscript for important intellectual content, and provided final approval of the submitted manuscript.

**Funding** 1R35HL139726-01, 1 R33 HL157907-01, R01HL144943.

## Declarations

**Conflict of Interest** The authors declare that they have no conflict of interest.

## References

1. Matthay MA, Zemans RL, Zimmerman GA et al (2019) Acute respiratory distress syndrome. Nat Rev Dis Primers 5:18
2. Wang D, Hu B, Hu C et al (2020) Clinical characteristics of 138 hospitalized patients with 2019 novel coronavirus-infected pneumonia in Wuhan, China. JAMA: 323(11):1061–1069. https://doi.org/10.1001/jama.2020.1585
3. Channappanavar R, Perlman S (2017) Pathogenic human coronavirus infections: causes and consequences of cytokine storm and immunopathology. Semin Immunopathol 39:529–539
4. Calfee CS, Delucchi KL, Sinha P et al (2018) Acute respiratory distress syndrome subphenotypes and differential response to simvastatin: secondary analysis of a randomised controlled trial. Lancet Respir Med 6:691–698
5. Sinha P, Delucchi KL, Thompson BT, McAuley DF, Matthay MA, Calfee CS (2018) Latent class analysis of ARDS subphenotypes: a secondary analysis of the statins for acutely injured lungs from sepsis (SAILS) study. Intensive Care Med 44:1859–1869
6. Calfee CS, Delucchi K, Parsons PE, Thompson BT, Ware LB, Matthay MA (2014) Subphenotypes in acute respiratory distress syndrome: latent class analysis of data from two randomised controlled trials. Lancet Respir Med 2:611–620
7. Chow CW, Herrera Abreu MT, Suzuki T, Downey GP (2003) Oxidative stress and acute lung injury. Am J Respir Cell Mol Biol 29:427–431
8. Kellner M, Noonepalle S, Lu Q, Srivastava A, Zemskov E, Black SM (2017) ROS signaling in the pathogenesis of Acute Lung Injury (ALI) and Acute Respiratory Distress Syndrome (ARDS). Adv Exp Med Biol 967:105–137
9. Taher A, Lashgari M, Sedighi L, Rahimi-Bashar F, Poorolajal J, Mehrpooya M (2021) A pilot study on intravenous N-Acetylcysteine treatment in patients with mild-to-moderate COVID19-associated acute respiratory distress syndrome. Pharmacol Rep 73:1650–1659
10. Obi J, Pastores SM, Ramanathan LV, Yang J, Halpern NA (2020) Treating sepsis with vitamin C, thiamine, and hydrocortisone: exploring the quest for the magic elixir. J Crit Care 57:231–239
11. Bernard GR, Wheeler AP, Arons MM et al (1997) A trial of antioxidants N-acetylcysteine and procysteine in ARDS. The antioxidant in ARDS study group. Chest 112:164–172
12 Dushianthan A, Cusack R, Burgess VA, Grocott MP, Calder PC (2019) Immunonutrition for acute respiratory distress syndrome (ARDS) in adults. Cochrane Database Syst Rev 1:Cd012041
13. Fowler AA 3rd, Truwit JD, Hite RD et al (2019) Effect of vitamin C infusion on organ failure and biomarkers of inflammation and vascular injury in patients with sepsis and severe acute respiratory failure: the CITRIS-ALI randomized clinical trial. JAMA 322:1261–1270
14. Langlois PL, D'Aragon F, Hardy G, Manzanares W (2019) Omega-3 polyunsaturated fatty acids in critically ill patients with acute respiratory distress syndrome: a systematic review and meta-analysis. Nutrition 61:84–92
15. Mahmoodpoor A, Hamishehkar H, Shadvar K et al (2019) The effect of intravenous selenium on oxidative stress in critically ill patients with acute respiratory distress syndrome. Immunol Invest 48:147–159
16. Alonso de Vega JM, Díaz J, Serrano E, Carbonell LF (2002) Oxidative stress in critically ill patients with systemic inflammatory response syndrome. Crit Care Med 30:1782–1786
17. Forman HJ, Zhang H (2021) Targeting oxidative stress in disease: promise and limitations of antioxidant therapy. Nat Rev Drug Discovery 20:689–709
18. Dikalov S, Fink B, Skatchkov M, Bassenge E (1999) Comparison of glyceryl trinitrate-induced with pentaerythrityl tetranitrate-induced in vivo formation of superoxide radicals: effect of vitamin C. Free Radic Biol Med 27:170–176
19. Dikalov SI, Dikalova AE, Morozov DA, Kirilyuk IA (2018) Cellular accumulation and antioxidant activity of acetoxymethoxycarbonyl pyrrolidine nitroxides. Free Radic Res 52:339–350
20. Carlsson LM, Jonsson J, Edlund T, Marklund SL (1995) Mice lacking extracellular superoxide dismutase are more sensitive to hyperoxia. Proc Natl Acad Sci U S A 92:6264–6268
21. Folz RJ, Abushamaa AM, Suliman HB (1999) Extracellular superoxide dismutase in the airways of transgenic mice reduces inflammation and attenuates lung toxicity following hyperoxia. J Clin Invest 103:1055–1066
22. Elajaili HB, Dee N, Woodcock L et al (2022) Developing EPR Tools for Preclinical Interrogation of Redox Regulation Mechanisms Contributing to Acute Lung Injury. In B50 Diffuse Lung Disease and Acute Lung Injury. American Thoracic Society, pp. A3018-A3018
23. Fink B, Dikalov S, Bassenge E (2000) A new approach for extracellular spin trapping of nitroglycerin-induced superoxide radicals both in vitro and in vivo. Free Radical Biol Med 28:121–128
24. Ahmed MN, Zhang Y, Codipilly C et al (2012) Extracellular superoxide dismutase overexpression can reverse the course of hypoxia-induced pulmonary hypertension. Mol Med 18:38–46
25. Auten RL, O'Reilly MA, Oury TD, Nozik-Grayck E, Whorton MH (2006) Transgenic extracellular superoxide dismutase protects postnatal alveolar epithelial proliferation and development during hyperoxia. Am J Physiol Lung Cell Mol Physiol 290:L32-40

26. Kang SK, Rabbani ZN, Folz RJ et al (2003) Overexpression of extracellular superoxide dismutase protects mice from radiation-induced lung injury. Int J Radiat Oncol Biol Phys 57:1056–1066
27. Nozik-Grayck E, Suliman HB, Majka S et al (2008) Lung EC-SOD overexpression attenuates hypoxic induction of Egr-1 and chronic hypoxic pulmonary vascular remodeling. Am J Physiol Lung Cell Mol Physiol 295:L422-430
28. Perveen S, Patel H, Arif A, Younis S, Codipilly CN, Ahmed M (2012) Role of EC-SOD overexpression in preserving pulmonary angiogenesis inhibited by oxidative stress. PLoS One 7:e51945
29. Rabbani ZN, Anscher MS, Folz RJ et al (2005) Overexpression of extracellular superoxide dismutase reduces acute radiation induced lung toxicity. BMC Cancer 5:59
30. Suliman HB, Ryan LK, Bishop L, Folz RJ (2001) Prevention of influenza-induced lung injury in mice overexpressing extracellular superoxide dismutase. Am J Physiol Lung Cell Mol Physiol 280:L69-78
31. Zaghloul N, Nasim M, Patel H et al (2012) Overexpression of extracellular superoxide dismutase has a protective role against hyperoxia-induced brain injury in neonatal mice. FEBS J 279:871–881
32. Suliman HB, Ali M, Piantadosi CA (2004) Superoxide dismutase-3 promotes full expression of the EPO response to hypoxia. Blood 104:43–50
33. Kliment CR, Suliman HB, Tobolewski JM et al (2009) Extracellular superoxide dismutase regulates cardiac function and fibrosis. J Mol Cell Cardiol 47:730–742
34. Lee YS, Cheon IS, Kim BH, Kwon MJ, Lee HW, Kim TY (2013) Loss of extracellular superoxide dismutase induces severe IL-23-mediated skin inflammation in mice. J Invest Dermatol 133:732–741
35. Manni ML, Tomai LP, Norris CA et al (2011) Extracellular superoxide dismutase in macrophages augments bacterial killing by promoting phagocytosis. Am J Pathol 178:2752–2759
36. Nozik-Grayck E, Woods C, Taylor JM et al (2014) Selective depletion of vascular EC-SOD augments chronic hypoxic pulmonary hypertension. Am J Physiol Lung Cell Mol Physiol 307:L868-876
37. Rola R, Zou Y, Huang TT et al (2007) Lack of extracellular superoxide dismutase (EC-SOD) in the microenvironment impacts radiation-induced changes in neurogenesis. Free Radic Biol Med 42:1133–1145 (discussion 1131-1132)
38. Zelko IN, Folz RJ (2010) Extracellular superoxide dismutase attenuates release of pulmonary hyaluronan from the extracellular matrix following bleomycin exposure. FEBS Lett 584:2947–2952
39. Kusuyama J, Alves-Wagner AB, Conlin RH et al (2021) Placental superoxide dismutase 3 mediates benefits of maternal exercise on offspring health. Cell Metab 33:939-956.e938
40. Yang R, Wei L, Fu QQ, Wang H, You H, Yu HR (2016) SOD3 ameliorates H2O2-induced oxidative damage in SH-SY5Y cells by inhibiting the mitochondrial pathway. Neurochem Res 41:1818–1830
41. Ueda J, Starr ME, Takahashi H et al (2008) Decreased pulmonary extracellular superoxide dismutase during systemic inflammation. Free Radical Biol Med 45:897–904
42. Fu C, Dai X, Yang Y, Lin M, Cai Y, Cai S (2017) Dexmedetomidine attenuates lipopolysaccharide-induced acute lung injury by inhibiting oxidative stress, mitochondrial dysfunction and apoptosis in rats. Mol Med Rep 15:131–138
43. Zielonka J, Kalyanaraman B (2010) Hydroethidine- and MitoSOX-derived red fluorescence is not a reliable indicator of intracellular superoxide formation: another inconvenient truth. Free Radic Biol Med 48:983–1001
44. Proniewski B, Kij A, Sitek B, Kelley EE, Chlopicki S (2019) Multiorgan development of oxidative and nitrosative stress in LPS-induced endotoxemia in C57Bl/6 mice: DHE-based *In Vivo* approach. Oxid Med Cell Longev 2019:7838406
45. Kozlov AV, Szalay L, Umar F et al (2003) Epr analysis reveals three tissues responding to endotoxin by increased formation of reactive oxygen and nitrogen species. Free Radic Biol Med 34:1555–1562
46. Elajaili H, Hernandez-Lagunas L, Harris P et al (2022) Extracellular superoxide dismutase (EC-SOD) R213G variant reduces mitochondrial ROS and preserves mitochondrial function in bleomycin-induced lung injury: EC-SOD R213G variant and intracellular redox regulation. Adv Redox Res 5:100035
47. Halpern HJ, Bowman MK (1991) Low-frequency EPR spectrometers: MHz range. In: Eaton GR, Eaton SS, Ohno K (eds) EPR Imaging and In Vivo EPR. CRC Press, Boca Raton, ch. 6
48. Rinard GA, Quine RW, Eaton SS, Eaton GR (2002) Frequency dependence of EPR signal intensity, 250 MHz to 9.1 GHz. J Magn Reson 156:113–121